

Lepton flavor-violating processes in the simplest little Higgs model: $e^+e^-(\gamma\gamma) \rightarrow l_i\bar{l}_j$ under new bound from $l_i \rightarrow l_j\gamma$

Lei Wang and Xiao-Fang Han*

Department of Physics, Yantai University, Yantai 264005, China

(Received 14 October 2011; published 13 January 2012)

We study the lepton flavor-violating processes in the simplest little Higgs model. First, we examine the constraints on the relevant parameters from the rare decays $l_i \rightarrow l_j\gamma$ ($i \neq j$ and $l_i = e, \mu, \tau$), especially for the latest data of $Br(\mu \rightarrow e\gamma)$. Then, we calculate the lepton flavor-violating processes $e^+e^- \rightarrow l_i\bar{l}_j$ and $\gamma\gamma \rightarrow l_i\bar{l}_j$ at the International Linear Collider and find that the simplest little Higgs model can produce significant contributions to these processes. The rates of $\gamma\gamma \rightarrow l_i\bar{l}_j$ can reach $\mathcal{O}(1)$ fb in the parameter space allowed by the experimental data, which implies that these processes may be observed at the International Linear Collider.

DOI: 10.1103/PhysRevD.85.013011

PACS numbers: 13.35.-r, 11.30.Fs, 12.60.-i, 13.66.De

I. INTRODUCTION

Little Higgs theory [1] has been proposed as an interesting solution to the hierarchy problem. So far, various realizations of the little Higgs symmetry structure have been proposed [2–5], which can be categorized generally into two classes [6]. One class uses the product group, represented by the littlest Higgs model [3], in which the standard model (SM) $SU(2)_L$ gauge group is from the diagonal breaking of two (or more) gauge groups. The other class uses the simple group, represented by the simplest little Higgs model (SLHM) [4], in which a single larger gauge group is broken down to the SM $SU(2)_L$. The flavor sector of little Higgs models based on product groups, notably the littlest Higgs model with T-parity (LHT) [5], has been extensively studied [7,8]. Recently, some attention has been paid to the flavor sector of SLHM [9–11].

The lepton flavor-violating (LFV) processes are extremely suppressed in the SM but can be greatly enhanced in new physics models. Therefore, the LFV processes can be a sensitive probe for new physics, which have been studied in R-parity conserving minimal supersymmetric standard model (MSSM) [12,13], R-parity violating MSSM [14], topcolor-assisted technicolor (TC2) model [15], and LHT [8]. The SLHM predicts the existence of heavy neutrinos, which have flavor-changing couplings with the SM leptons mediated, respectively, by the SM gauge boson W^\pm and the new heavy gauge boson X^\pm . These couplings can give great contributions to LFV processes at the one-loop level.

The next generation e^+e^- International Linear Collider (ILC) with the center-of-mass energy $\sqrt{s} = 0.5\text{--}1$ TeV and the integrated luminosity $\mathcal{L}_{\text{int}} = 500 \text{ fb}^{-1}$ with the first four years is currently being designed [16,17]. In such a collider, in addition to e^+e^- collision, one can also realize $\gamma\gamma$ collision with the photon beams generated by the backward Compton scattering of incident electron

and laser beams. Because of its rather clean environment and high luminosity, the ILC can precisely measure the LFV processes $e^+e^- \rightarrow l_i\bar{l}_j$ and $\gamma\gamma \rightarrow l_i\bar{l}_j$ ($i \neq j$ and $l_i = e, \mu, \tau$). Very recently, the MEG Collaboration presented the upper limit of 2.4×10^{-12} on the branching ratio of the $\mu \rightarrow e\gamma$ decay, constituting the most stringent limit on the existence of this decay to date [18]. The upper bounds on $Br(\tau \rightarrow e\gamma)$ and $Br(\tau \rightarrow \mu\gamma)$ are respectively 1.1×10^{-7} and 4.5×10^{-8} [19]. In the framework of SLHM, we study the $e^+e^- \rightarrow l_i\bar{l}_j$ and $\gamma\gamma \rightarrow l_i\bar{l}_j$ at the ILC, taking into account the constraints from $l_i \rightarrow l_j\gamma$ decay.

This work is organized as follows. In Sec. II, we recapitulate the SLHM. In Secs. III and IV, we study, respectively, the LFV processes $l_i \rightarrow l_j\gamma$, $e^+e^- \rightarrow l_i\bar{l}_j$ and $\gamma\gamma \rightarrow l_i\bar{l}_j$. Finally, we give our conclusion in Sec. V.

II. SIMPLEST LITTLE HIGGS MODEL

The SLHM is based on $[SU(3) \times U(1)_X]^2$ global symmetry [4]. The gauge symmetry $SU(3) \times U(1)_X$ is broken down to the SM electroweak gauge group by two copies of scalar fields Φ_1 and Φ_2 , which are triplets under the $SU(3)$ with aligned vacuum expectation values (VEVs) f_1 and f_2 . The uneaten five pseudo-Goldstone bosons can be parameterized as

$$\Phi_1 = e^{it_\beta\Theta} \begin{pmatrix} 0 \\ 0 \\ f_1 \end{pmatrix}, \quad \Phi_2 = e^{-(i/t_\beta)\Theta} \begin{pmatrix} 0 \\ 0 \\ f_2 \end{pmatrix}, \quad (1)$$

where

$$\Theta = \frac{1}{f} \left[\begin{pmatrix} 0 & 0 & H \\ 0 & 0 & 0 \\ H^\dagger & 0 & 0 \end{pmatrix} + \frac{\eta}{\sqrt{2}} \begin{pmatrix} 1 & 0 & 0 \\ 0 & 1 & 0 \\ 0 & 0 & 1 \end{pmatrix} \right], \quad (2)$$

$f = \sqrt{f_1^2 + f_2^2}$ and $t_\beta \equiv \tan\beta = f_2/f_1$. Under the $SU(2)_L$ SM gauge group, η is a real scalar, while H transforms as a doublet and can be identified as the SM Higgs doublet. The kinetic term in the nonlinear sigma model is

*xfhan@itp.ac.cn

$$\mathcal{L}_\Phi = \sum_{j=1,2} \left| \left(\partial_\mu + igA_\mu^a T^a - i \frac{g_x}{3} B_\mu^x \right) \Phi_j \right|^2, \quad (3)$$

where $g_x = gt_W/\sqrt{1-t_W^2/3}$, and $t_W = \tan\theta_W$ with θ_W being the electroweak mixing angle. As Φ_1 and Φ_2 develop their vacuum expectation values, the new heavy gauge bosons Z' , Y^0 , $Y^{0\dagger}$ and X^\pm get their masses after eating five Goldstone bosons,

$$\begin{aligned} M_X &= \frac{gf}{\sqrt{2}} \left(1 - \frac{v^2}{4f^2} \right), \\ M_{Z'} &= \frac{\sqrt{2}gf}{\sqrt{3-t_W^2}} \left(1 - \frac{3-t_W^2}{c_W^2} \frac{v^2}{16f^2} \right), \\ M_Y &= \frac{gf}{\sqrt{2}}. \end{aligned} \quad (4)$$

The gauged $SU(3)$ symmetry promotes the SM fermion doublets into $SU(3)$ triplets. For each generation of lepton, a heavy neutrino is added, whose mass is

$$m_{N_i} = fs_\beta \lambda_N^i, \quad (5)$$

where $i = 1, 2, 3$ is the generation index and λ_N^i is the Yukawa coupling constant.

After the electroweak symmetry breaking (EWSB), the light and the heavy neutrino of the same family have the mixing, which is parameterized by $\delta_\nu = -\frac{v}{\sqrt{2}ft_\beta}$. The mixing angle δ_ν is experimentally constrained to be small [20] and taken as a typical upper limit $\delta_\nu < 0.05$ following Ref. [9]. Besides, there is family mixing as long as the Yukawa matrix of heavy neutrinos and that of leptons are not aligned. This can induce the lepton flavor-changing interactions of charged currents proportional to $V_\ell^{ij} \bar{N}_i \gamma^\mu X^{+\mu} l_j$ and $\delta_\nu V_\ell^{ij} \bar{N}_i \gamma^\mu W^{+\mu} l_j$, where V_ℓ^{ij} is the mixing matrix [6,9,10].

III. THE LFV PROCESSES $\mu \rightarrow e\gamma$ AND $e^+e^- \rightarrow l_i \bar{l}_j$

In our calculation, we take the 't Hooft-Feynman gauge. The flavor-changing interactions between the heavy neutrino and lepton, mediated by the gauge bosons (corresponding Goldstone bosons) X^\pm (x^\pm) and W^\pm (ϕ^\pm), can contribute to these decays. The relevant Feynman rules can be found in Ref. [9], and the Feynman diagrams for $e^+e^- \rightarrow l_i \bar{l}_j$ can be depicted by Fig. 1. The SLHM can contribute to the LFV processes $e^+e^- \rightarrow l_i \bar{l}_j$ via the effective vertices $\gamma l_i \bar{l}_j$, $Z l_i \bar{l}_j$, $Z' l_i \bar{l}_j$, and the box diagrams. The calculations of the loop diagrams in Fig. 1 are straightforward. Each loop diagram is composed of some scalar loop functions [21], which are calculated by using LOOPTOOLS [22]. The calculations are tedious, and the analytical expressions are lengthy, which are not presented here.

Very recently, the MEG Collaboration presented the upper limit of 2.4×10^{-12} on the branching ratio of the $\mu \rightarrow e\gamma$ decay, constituting the most stringent limit

on the existence of this decay to date [18]. The upper bounds on $Br(\tau \rightarrow e\gamma)$ and $Br(\tau \rightarrow \mu\gamma)$ are, respectively, 1.1×10^{-7} and 4.5×10^{-8} [19]. The $l_i \rightarrow l_j \gamma$ can be depicted by the effective vertex $\gamma l_i \bar{l}_j$ involved in Fig. 1.

We take $\mu \rightarrow e\gamma$ as an example to show analytic results. The partial width for $\mu \rightarrow e\gamma$ can be expressed in terms of the dipole form factors of the lepton flavor-changing one-loop vertex as [9]:

$$\Gamma(\mu \rightarrow e\gamma) = \frac{\alpha}{2} m_\mu^3 (|F_M^\gamma|^2 + |F_E^\gamma|^2), \quad (6)$$

where

$$\begin{aligned} F_M^\gamma &= -iF_E^\gamma \\ &= \frac{\alpha}{16\pi s_W^2} \frac{m_\mu}{M_W^2} \sum_{i=1,2,3} V_\ell^{ie*} V_\ell^{i\mu} \left[\frac{v^2}{2f^2} F_X(x_i) \right. \\ &\quad \left. + \delta_\nu^2 F_W(x_i/\omega) \right], \end{aligned} \quad (7)$$

$$\text{with } x_i = \frac{m_{N_i}^2}{M_X^2}, \omega = \frac{M_W^2}{M_X^2},$$

$$\begin{aligned} F_X(x) &= \frac{5}{6} - \frac{3x - 15x^2 - 6x^3}{12(1-x)^3} + \frac{3x^3}{2(1-x)^4} \ln x, \\ F_W(x) &= \frac{x(-7 + 5x + 8x^2)}{12(1-x)^3} + \frac{x^2(-2 + 3x)}{2(1-x)^4} \ln x. \end{aligned} \quad (8)$$

The SM input parameters relevant in our study are taken as Ref. [23]. The free SLHM parameters involved are f , t_β , the heavy neutrino mass m_{N_i} ($i = 1, 2, 3$), and the mixing matrix V_ℓ . To simplify our calculations, we assume the heavy neutral lepton mass basis is aligned with the SM neutrino mass basis, which induces V_ℓ to be equal to the Pontcove-Mkai-Nagawa-Sakata neutrino mixing matrix. Thus, the matrix V_ℓ can be parameterized with standard form, and we take the parameters [24]

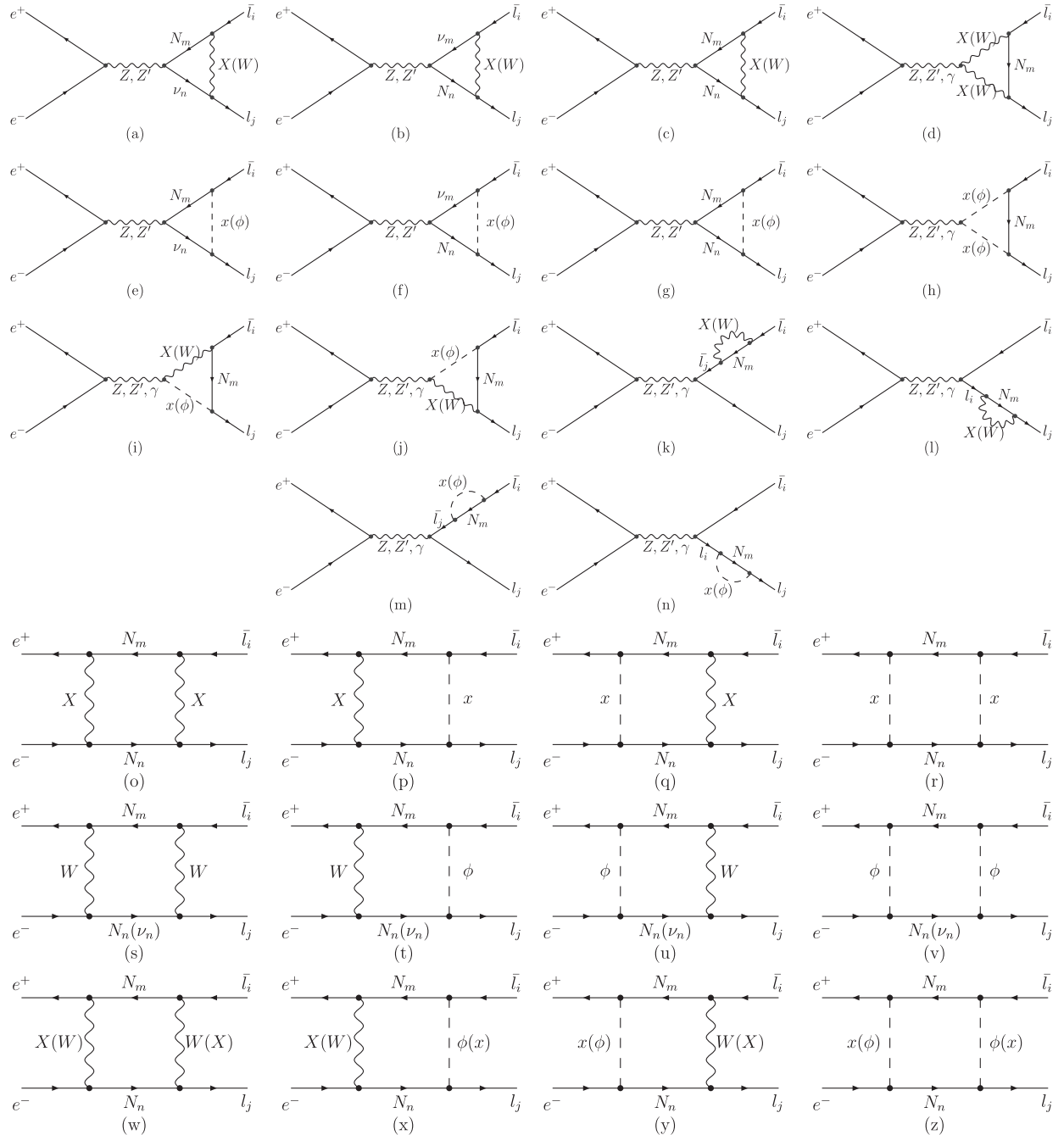
$$\begin{aligned} s_{12} &= \sqrt{0.3}, & s_{13} &= \sqrt{0.03}, \\ s_{23} &= \frac{1}{\sqrt{2}}, & \delta_{13} &= 65^\circ, \end{aligned} \quad (9)$$

which is consistent with the experimental constraints on the Pontcove-Mkai-Nagawa-Sakata matrix [25], and δ_{13} is taken to be equal to the Cabibbo-Kobayashi-Maskawa phase. We assume that the heavy neutrino masses of the first two generations are degenerate and take $m_{N_1} = m_{N_2} = m_1 = 400$ GeV.

In Fig. 2, we scan the following parameter space:

$$\begin{aligned} 1 \text{ TeV} < f < 6 \text{ TeV}, \quad 1 < t_\beta < 15, \\ 0.5 \text{ TeV} < m_3 < 3 \text{ TeV}, \end{aligned} \quad (10)$$

and plot, respectively, the decay branching ratio of $\mu \rightarrow e\gamma$ versus f and m_3 under the constraints of $Br(\tau \rightarrow e\gamma)$ and

FIG. 1. Feynman diagrams for $e^+e^- \rightarrow l_i\bar{l}_j$ in the SLHM.

$Br(\tau \rightarrow \mu\gamma)$. We find that the branching ratio drops as the scale f gets large, and the reason is that the lepton flavor-changing couplings $\bar{N}_i \gamma^\mu W^{+\mu} l_j$ and $\bar{N}_i \phi^+ l_j$ are proportional to $\delta_\nu = -\frac{v}{\sqrt{2} f t_\beta}$. Besides, the branching ratio increases with the mass of the third-generation heavy neutrino. The reason is that the decay width of $\mu \rightarrow e\gamma$ is enhanced by the large mass splitting $m_3 - m_1$, which increases with m_3 since we have fixed the value of m_1 . More specifically, due to the unitarity of the mixing matrix V_ℓ , the decay width of $\mu \rightarrow e\gamma$ shown in Eqs. (6) and (7)

equals to zero for the degenerate heavy neutrino masses of the three generations, i.e. $x_1 = x_2 = x_3$. In our calculations, we fix $x_1 = x_2$, which can induce

$$\begin{aligned} \sum_{i=1,2} V_\ell^{ie*} V_\ell^{i\mu} & \left[\frac{v^2}{2f^2} F_X(x_i) + \delta_\nu^2 F_W(x_i/\omega) \right] \\ & = -V_\ell^{3e*} V_\ell^{3\mu} \left[\frac{v^2}{2f^2} F_X(x_1) + \delta_\nu^2 F_W(x_1/\omega) \right]. \end{aligned} \quad (11)$$

Thus, Eq. (7) can be written as

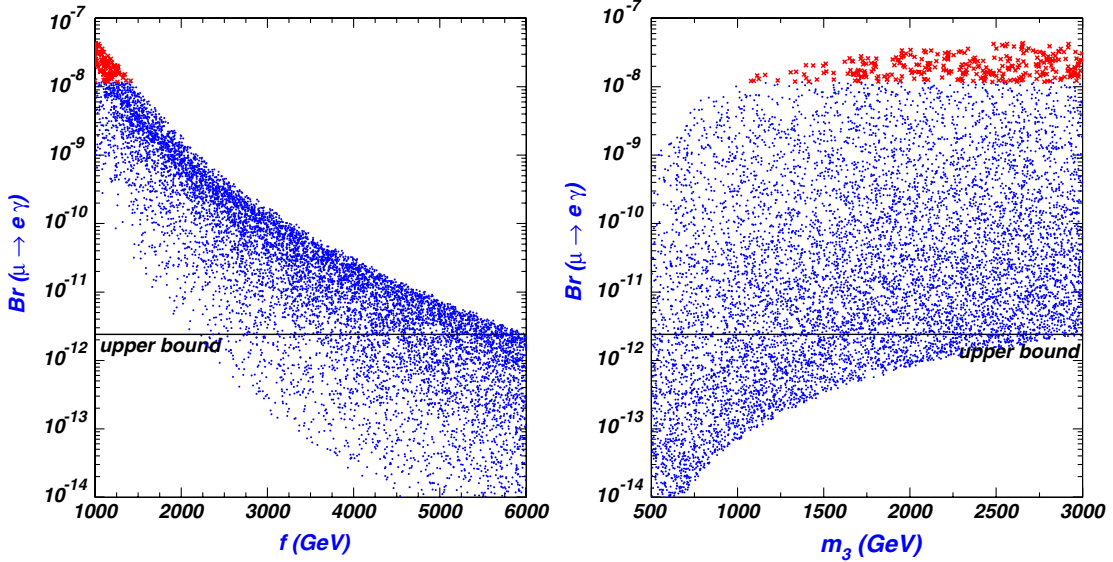


FIG. 2 (color online). Scatter plots for $Br(\mu \rightarrow e\gamma)$ versus f and m_3 , respectively. The bullets (blue) and the crosses (red) are allowed and excluded by the upper bounds of $Br(\tau \rightarrow e\gamma)$ and $Br(\tau \rightarrow \mu\gamma)$, respectively.

$$\begin{aligned} F_M^\gamma &= -iF_E^\gamma \\ &= \frac{\alpha}{16\pi s_W^2 M_W^2} \frac{m_\mu}{V_\ell^{3e*} V_\ell^{3\mu}} \left[\frac{v^2}{2f^2} F_X(x_3) + \delta_\nu^2 F_W(x_3/\omega) \right. \\ &\quad \left. - \frac{v^2}{2f^2} F_X(x_1) - \delta_\nu^2 F_W(x_1/\omega) \right]. \end{aligned} \quad (12)$$

The functions $F_X(x)$ and $F_W(x)$ will decrease as x increases. However, when x is much larger than 1, $F_X(x)$ and $F_W(x)$ are no longer sensitive to x and, respectively, approach the limits $\frac{1}{3}$ and $-\frac{2}{3}$. Therefore, with $m_{N_1} = m_{N_2} = m_1 = 400$ GeV being fixed, Eq. (6) and Eq. (12) show the decay width of $\mu \rightarrow e\gamma$ will increase as m_3 gets

large, but approach a limit where m_3 is much larger than m_X .

Figure 2 shows the experimental data of $Br(\mu \rightarrow e\gamma)$ favors $f > 2$ TeV and $m_3 < 2.5$ TeV with $m_{N_1} = m_{N_2} = m_1 = 400$ GeV. Compared to the $Br(\mu \rightarrow e\gamma)$, the lesser region of the parameter space scanned is not allowed by the upper bounds of $Br(\tau \rightarrow e\gamma)$ and $Br(\tau \rightarrow \mu\gamma)$. This shows that the upper bound of $Br(\mu \rightarrow e\gamma)$ can give more strong constraints on the relevant parameters than those of $Br(\tau \rightarrow e\gamma)$ and $Br(\tau \rightarrow \mu\gamma)$ for the values of V_ℓ and the heavy neutrino masses of the first two generations taken in our calculations.

In Figs. 3–5, we plot, respectively, the cross sections of $e^+ e^- \rightarrow \bar{\mu}e$, $e^+ e^- \rightarrow \bar{\tau}e$ and $e^+ e^- \rightarrow \bar{\tau}\mu$ versus m_3 in

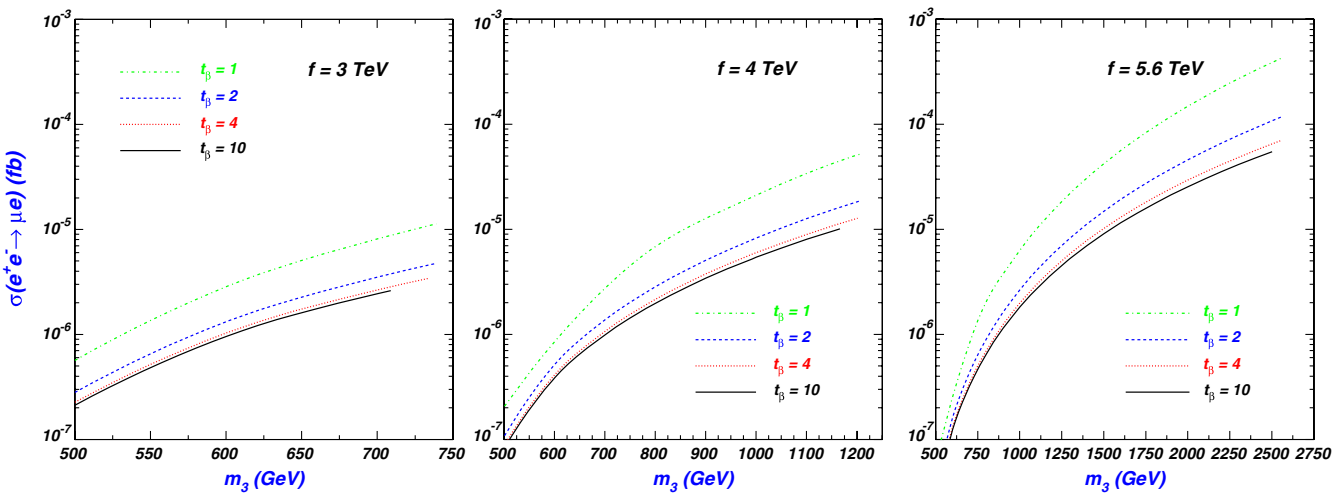
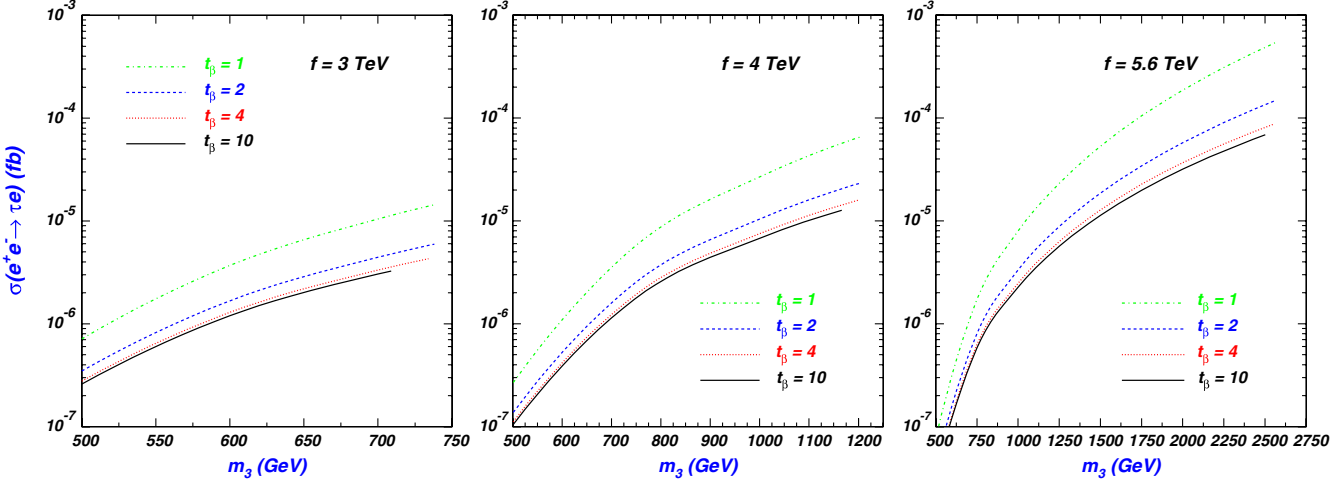
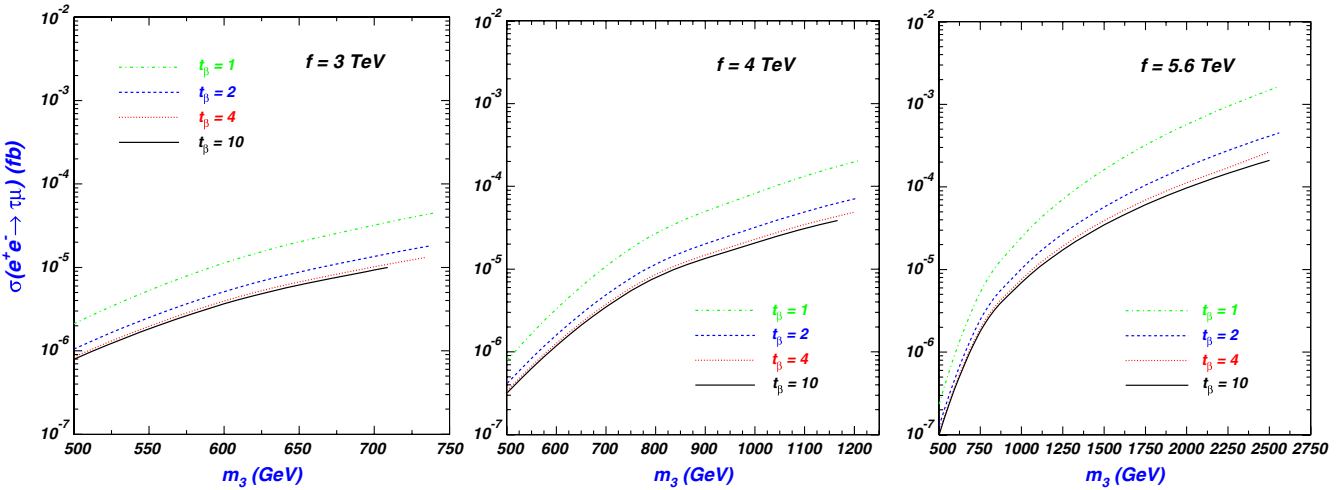


FIG. 3 (color online). The cross section of $e^+ e^- \rightarrow \bar{\mu}e$ versus m_3 . The incomplete lines for the values of t_β show, respectively, the upper bounds of m_3 given by the experimental data of $Br(l_i \rightarrow l_j \gamma)$. In fact, $f = 3$ TeV, and $t_\beta = 1$ is not allowed by the upper limit $\delta_\nu = -\frac{v}{\sqrt{2}f t_\beta} < 0.05$ mentioned in Sec. II.

FIG. 4 (color online). Same as Fig. 3, but for $e^+e^- \rightarrow \bar{\tau}e$.FIG. 5 (color online). Same as Fig. 3, but for $e^+e^- \rightarrow \bar{\tau}\mu$.

the parameter space allowed by the experimental data of $l_i \rightarrow l_j \gamma$. The upper bounds of m_3 are, respectively, about 725 GeV, 1200 GeV, and 2500 GeV for $f = 3$ TeV, $f = 4$ TeV, and $f = 5.6$ TeV with $m_{N_1} = m_{N_2} = m_1 = 400$ GeV. Compared to the SM predictions, SLHM can enhance sizably the cross sections of the three LFV production processes, and the magnitude increases with m_3 . The cross sections can reach $\mathcal{O}(10^{-4})$ fb for $e^+e^- \rightarrow \bar{\mu}e$, $\mathcal{O}(10^{-4})$ fb for $e^+e^- \rightarrow \bar{\tau}e$, and $\mathcal{O}(10^{-3})$ fb for $e^+e^- \rightarrow \bar{\tau}\mu$. Such cross sections imply that it is challenging to detect the three LFV production processes at the ILC.

IV. THE LFV PROCESSES $\gamma\gamma \rightarrow l_i \bar{l}_j$

It is well-known that the ILC could offer the possibility of working in the $\gamma\gamma$ collision, thus realizing a high-energy photon collider [16,17]. The SLHM can induce the LFV

processes $\gamma\gamma \rightarrow l_i \bar{l}_j$ at loop level. The relevant Feynman diagrams are shown in Fig. 6.

Since the photon beams in $\gamma\gamma$ collision are generated by the backward Compton scattering of the incident electron and laser beam, the effective cross section of $\gamma\gamma \rightarrow l_i \bar{l}_j$ can be written as [26]

$$\begin{aligned} \sigma_{\gamma\gamma \rightarrow l_i \bar{l}_j}(s) &= \int_{\sqrt{s}}^{x_{\max}} 2z dz \hat{\sigma}_{\gamma\gamma \rightarrow l_i \bar{l}_j}(s_{\gamma\gamma}) \\ &= z^2 s \int_{z^2/x_{\max}}^{x_{\max}} \frac{dx}{x} F_{\gamma/e}(x) F_{\gamma/e}\left(\frac{z^2}{x}\right), \end{aligned} \quad (13)$$

where s is the squared center-of-mass energy of e^+e^- collision. $F_{\gamma/e}$ denotes the energy spectrum of the back-scattered photon for the unpolarized initial electron and laser photon beams given by

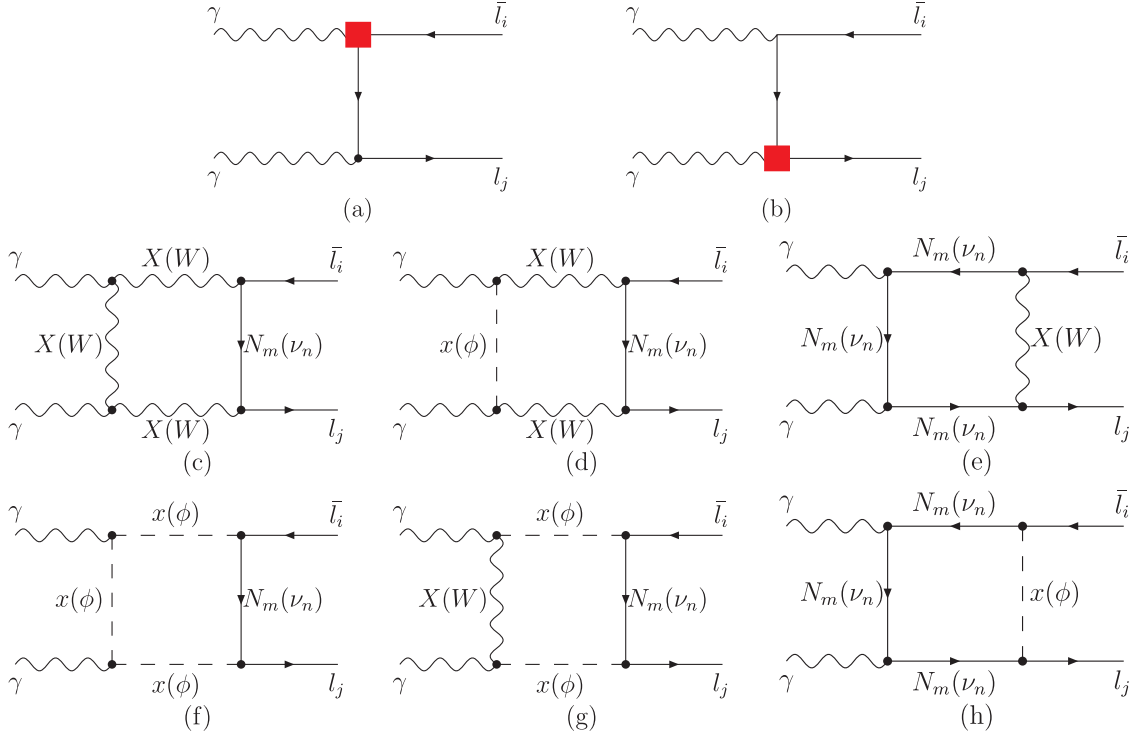


FIG. 6 (color online). Feynman diagrams for $\gamma\gamma \rightarrow l_i\bar{l}_j$ in the SLHM. The effective $\gamma l_i l_j$ vertex in (a, b) is shown in Fig. 1. The diagrams obtained by exchanging the initial photons are not shown here.

$$F_{\gamma/e}(x) = \frac{1}{D(\xi)} \left[1 - x + \frac{1}{1-x} - \frac{4x}{\xi(1-x)} + \frac{4x^2}{\xi^2(1-x)^2} \right], \quad (14)$$

with

$$D(\xi) = \left(1 - \frac{4}{\xi} - \frac{8}{\xi^2} \right) \ln(1 + \xi) + \frac{1}{2} + \frac{8}{\xi} - \frac{1}{2(1 + \xi)^2}, \quad (15)$$

where $\xi = 4E_e E_0 / m_e^2$, with E_e being the incident electron energy and E_0 being the initial laser photon energy. x is the fraction of the energy of the incident electron carried by the back-scattered photon. In order to spoil the creation of e^+e^- pair by the interaction of the incident and back-scattered photons, we fix $\xi = 4.8$, $x_{\max} = 0.83$, and $D(\xi) = 1.8$ in our calculation [26].

Figures 7–9 show, respectively, the cross sections of $\gamma\gamma \rightarrow \bar{\mu}e$, $\gamma\gamma \rightarrow \bar{\tau}e$, and $\gamma\gamma \rightarrow \bar{\tau}\mu$ versus m_3 in the parameter space allowed by the experimental data of $l_i \rightarrow l_j \gamma$.

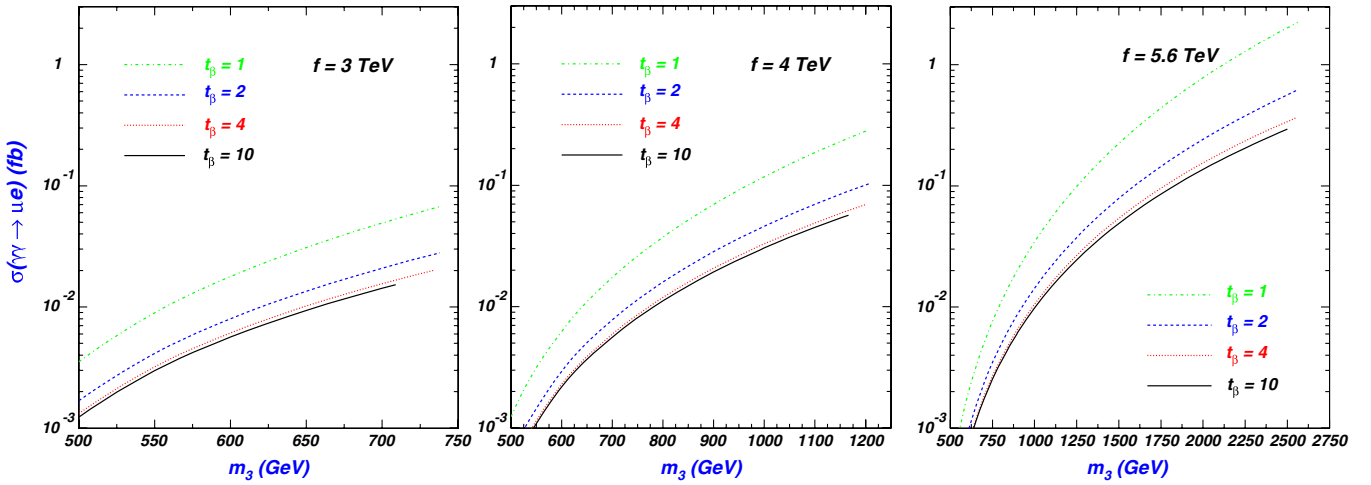
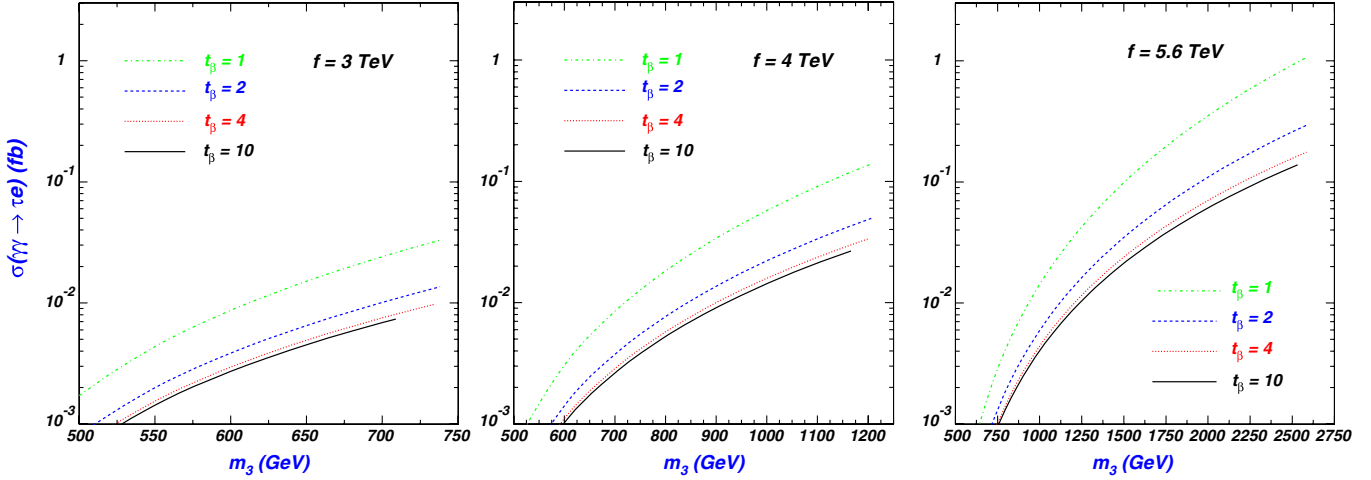
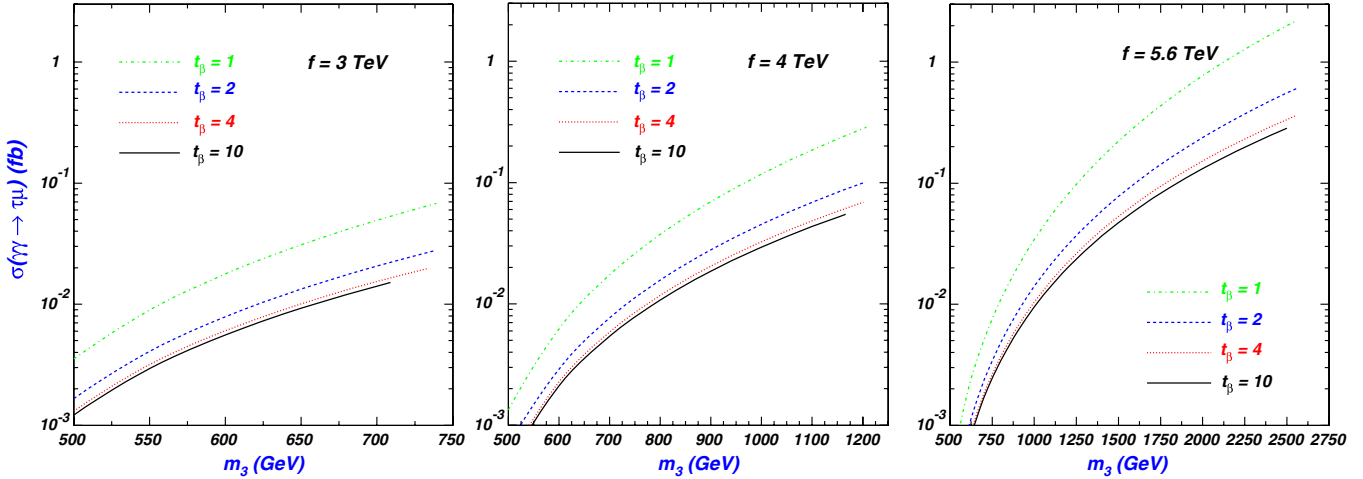


FIG. 7 (color online). Same as Fig. 3, but for $\gamma\gamma \rightarrow \bar{\mu}e$.

FIG. 8 (color online). Same as Fig. 3, but for $\gamma\gamma \rightarrow \bar{\tau}e$.FIG. 9 (color online). Same as Fig. 3, but for $\gamma\gamma \rightarrow \bar{\tau}\mu$.

We find the rates for $\gamma\gamma \rightarrow l_i \bar{l}_j$ can be several orders larger than those of $e^+ e^- \rightarrow l_i \bar{l}_j$, which can reach $\mathcal{O}(1)$ fb. The reason is that the processes $e^+ e^- \rightarrow l_i \bar{l}_j$ are *s*-channel suppressed, while the processes $\gamma\gamma \rightarrow l_i \bar{l}_j$ get contributions from *u*-channel and *t*-channel without such suppression.

Now, we discuss the observability of $\gamma\gamma \rightarrow l_i \bar{l}_j$ at the ILC. The $\gamma\gamma \rightarrow \bar{\mu}e$ is the best one and almost free of the SM backgrounds. For $\gamma\gamma \rightarrow \bar{\tau}e$, its main backgrounds come from $\gamma\gamma \rightarrow \tau^+ \tau^- \rightarrow \tau^- \nu_e \bar{\nu}_\tau e^+$, $\gamma\gamma \rightarrow W^+ W^- \rightarrow \tau^- \nu_e \bar{\nu}_\tau e^+$, and $\gamma\gamma \rightarrow e^+ e^- \tau^+ \tau^-$. With suitable cuts, the rates are 9.7×10^{-4} fb for $\gamma\gamma \rightarrow \tau^+ \tau^- \rightarrow \tau^- \nu_e \bar{\nu}_\tau e^+$,

0.1 fb for $\gamma\gamma \rightarrow W^+ W^- \rightarrow \tau^- \nu_e \bar{\nu}_\tau e^+$, and 0.024 fb for $\gamma\gamma \rightarrow e^+ e^- \tau^+ \tau^-$, respectively [13]. This implies the production rate for $\gamma\gamma \rightarrow \bar{\tau}e$ must be larger than 2.5×10^{-2} fb to get a 3σ observing sensitivity with 3.45×10^{-2} fb⁻¹ integrated luminosity [27]. The backgrounds for the $\gamma\gamma \rightarrow \bar{\tau}\mu$ are similar to those of $\gamma\gamma \rightarrow \bar{\tau}e$. The Figs. 7–9 show the processes $\gamma\gamma \rightarrow l_i \bar{l}_j$ at the ILC may be observable in the broad regions of the SLHM parameter space.

In Table I, we also list the production rates of $\gamma\gamma \rightarrow l_i \bar{l}_j$ in the optimum case of different models. We can find

TABLE I. The production rates for $\gamma\gamma \rightarrow l_i \bar{l}_j$ at the ILC with $\sqrt{s} = 500$ GeV in the optimum case of different models.

MSSM with R-parity	MSSM without R-parity	TC2	LHT	SLHM
$\gamma\gamma \rightarrow \bar{\tau}\mu$	$\mathcal{O}(10^{-2})$ [13]	$\mathcal{O}(10^{-2})$ [14]	$\mathcal{O}(1)$ [15]	$\mathcal{O}(1)$ [8]
$\gamma\gamma \rightarrow \bar{\tau}e$	$\mathcal{O}(10^{-1})$ [13]	$\mathcal{O}(10^{-2})$ [14]	$\mathcal{O}(1)$ [15]	$\mathcal{O}(10^{-1})$ [8]
$\gamma\gamma \rightarrow \bar{\mu}e$	$\mathcal{O}(10^{-3})$ [13]	$\mathcal{O}(10^{-4})$ [14]	$\mathcal{O}(10^{-3})$ [15]	$\mathcal{O}(10^{-1})$ [8]

that, since different models predict different patterns of the rates and the differences are sizable, the measurement of $\gamma\gamma \rightarrow l_i\bar{l}_j$ at the ILC may be utilized to distinguish the models.

V. CONCLUSION

We studied the LFV processes in the framework of the simplest little Higgs model. First, we examined the constraints of $Br(l_i \rightarrow l_j \gamma)$ on the model and found that $f > 2$ TeV and $m_3 < 2.5$ TeV is favored for $m_{N_1} = m_{N_2} = m_1 = 400$ GeV. Then, we studied the LFV processes $e^+e^- \rightarrow \bar{\mu}e$, $e^+e^- \rightarrow \bar{\tau}e$, and $e^+e^- \rightarrow \bar{\tau}\mu$ at the ILC and found that it is challenging to detect the three LFV

processes at the ILC, although their production rates can be enhanced sizably by SLHM. Finally, we studied the LFV processes $\gamma\gamma \rightarrow \bar{\mu}e$, $\gamma\gamma \rightarrow \bar{\tau}e$, and $\gamma\gamma \rightarrow \bar{\tau}\mu$ at the ILC and found that their production rates can reach $\mathcal{O}(1)$ fb, which implies that the three LFV processes may be observed at the ILC.

ACKNOWLEDGMENTS

This work was supported in part by the National Natural Science Foundation of China (NNSFC) under Grant Nos. 11005089 and 11105116 and by the Foundation of Yantai University under Grant Nos. WL10B24 and WL09B31.

-
- [1] N. Arkani-Hamed, A. G. Cohen, and H. Georgi, *Phys. Lett. B* **513**, 232 (2001); N. Arkani-Hamed, A. G. Cohen, E. Katz, A. E. Nelson, T. Gregoire, and J. G. Wacker, *J. High Energy Phys.* **08** (2002) 021.
 - [2] D.E. Kaplan and M. Schmaltz, *J. High Energy Phys.* **10** (2003) 039; I. Low, W. Skiba, and D. Smith, *Phys. Rev. D* **66**, 072001 (2002); S. Chang and J.G. Wacker, *Phys. Rev. D* **69**, 035002 (2004); T. Gregoire, D.R. Smith, and J.G. Wacker, *Phys. Rev. D* **69**, 115008 (2004); W. Skiba and J. Terning, *Phys. Rev. D* **68**, 075001 (2003); S. Chang, *J. High Energy Phys.* **12** (2003) 057; H. Cai, H.-C. Cheng, and J. Terning, *J. High Energy Phys.* **05** (2009) 045; A. Freitas, P. Schwaller, and D. Wyler, *J. High Energy Phys.* **12** (2009) 027.
 - [3] N. Arkani-Hamed, A. G. Cohen, E. Katz, and A. E. Nelson, *J. High Energy Phys.* **07** (2002) 034.
 - [4] M. Schmaltz, *J. High Energy Phys.* **08** (2004) 056.
 - [5] H.C. Cheng and I. Low, *J. High Energy Phys.* **09** (2003) 051; *J. High Energy Phys.* **08** (2004) 061; H.C. Cheng, I. Low, and L.T. Wang, *Phys. Rev. D* **74**, 055001 (2006); J. Hubisz and P. Meade, *Phys. Rev. D* **71**, 035016 (2005).
 - [6] T. Han, H.E. Logan, and L.T. Wang, *J. High Energy Phys.* **01** (2006) 099.
 - [7] M. Blanke, A.J. Buras, A. Poschenrieder, S. Recksiegel, C. Tarantino, S. Uhlig, and A. Weiler, *J. High Energy Phys.* **01** (2007) 066; J. Hubisz, S.J. Lee, and G. Paz, *J. High Energy Phys.* **06** (2006) 041; T. Goto, Y. Okada, and Y. Yamamoto, *Phys. Lett. B* **670**, 378 (2009); A. Paul, I.I. Bigi, and S. Recksiegel, *Phys. Rev. D* **82**, 094006 (2010); F. Penunuri and F. Larios, *Phys. Rev. D* **79**, 015013 (2009); X.-F. Han, L. Wang, and J.M. Yang, *Phys. Rev. D* **78**, 075017 (2008); *Phys. Rev. D* **80**, 015018 (2009); S. Fajfer and J.F. Kamenik, *J. High Energy Phys.* **12** (2007) 074; C.-H. Chen, C.-Q. Geng, and T.-C. Yuan, *Phys. Lett. B* **655**, 50 (2007); A. Belyaev, C.-R. Chen, K. Tobe, and C.-P. Yuan, *Phys. Rev. D* **74**, 115020 (2006).
 - [8] W. Ma, C.-X. Yue, J. Zhang, and Y.-B. Sun, *Phys. Rev. D* **82**, 095010 (2010); J. Han, X. Wang, and B. Yang, *Nucl. Phys. B* **843**, 383 (2011).
 - [9] F. del Aguila, J.I. Illana, and M.D. Jenkins, *J. High Energy Phys.* **03** (2011) 080.
 - [10] J.I. Illana and M.D. Jenkins, *Acta Phys. Pol. B* **40**, 3143 (2009); F.d. Aguila, J.I. Illana, and M.D. Jenkins, *Nucl. Phys. B, Proc. Suppl.* **205-206**, 158 (2010).
 - [11] A. Abada, G. Bhattacharyya, and M. Losada, *Phys. Rev. D* **73**, 033006 (2006); A.G. Dias, C.A. de S. Pires, and P.S. Rodrigues da Silva, *Phys. Rev. D* **77**, 055001 (2008); G. Marandella, C. Schappacher, and A. Strumia, *Phys. Rev. D* **72**, 035014 (2005); L. Wang and X.-F. Han, *Nucl. Phys. B* **853**, 625 (2011); A. Gutierrez-Rodriguez, *Mod. Phys. Lett. A* **25**, 703 (2010); K. Cheung and J. Song, *Phys. Rev. D* **76**, 035007 (2007); W. Kilian, D. Rainwater, and J. Reuter, *Phys. Rev. D* **71**, 015008 (2005).
 - [12] S.-M. Wang *et al.*, *Phys. Rev. D* **74**, 057902 (2006).
 - [13] M. Cannoni, C. Carimalo, W. Da Silva, and O. Panella, *Phys. Rev. D* **72**, 115004 (2005).
 - [14] Junjie Cao, Lei Wu, and Jinmin Yang, *Nucl. Phys. B* **829**, 370 (2010).
 - [15] Guo-Li Liu, *arXiv:1002.0659*.
 - [16] T. Abe *et al.* (American Linear Collider Group), *arXiv: hep-ex/0106057*; J.A. Aguilar-Saavedra *et al.* (ECFA/DESY LC Physics Working Group), *arXiv:hep-ph/0106315*; Koh Abe *et al.* (ACFA Linear Collider Working Group), *arXiv:hep-ph/0109166*; ILC Technical Review Committee, Second Report, SLAC-R-606, 2003.
 - [17] G. Aarons *et al.* (ILC Collaboration), *arXiv:0709.1893*; Brau *et al.* (ILC Collaboration), *arXiv:0712.1950*.
 - [18] MEG collaboration, *Phys. Rev. Lett.* **107**, 171801 (2011).
 - [19] M. Ahmed *et al.* (MEGA Collaboration), *Phys. Rev. D* **65**, 112002 (2002); K. Abe *et al.* (Belle Collaboration), *Phys. Rev. Lett.* **92**, 171802 (2004).
 - [20] F. del Aguila, J.A. Aguilar-Saavedra, and J. de Blas, *Acta Phys. Pol. B* **40**, 2901 (2009); O.C.W. Kong, J. Korean Phys. Soc. **45**, S404 (2004); F. del Aguila, J. de Blas, and M. Perez-Victoria, *Phys. Rev. D* **78**, 013010 (2008).
 - [21] G. 't Hooft and M.J.G. Veltman, *Nucl. Phys.* **B153**, 365 (1979).
 - [22] T. Hahn and M. Perez-Victoria, *Comput. Phys. Commun.* **118**, 153 (1999); T. Hahn, *Nucl. Phys. B, Proc. Suppl.* **135**, 333 (2004).
 - [23] C. Amsler *et al.*, *Phys. Lett. B* **667**, 1 (2008).

- [24] O. Mena and S. J. Parke, Phys. Rev. D **69**, 117301 (2004); R.N. Mohapatra *et al.*, Rep. Prog. Phys. **70**, 1757 (2007); G. Ahuja, M. Gupta, and M. Randhawa, PU Research Journal (Science) **57**, 257 (2007).
- [25] S. Eidelman *et al.* (Particle Data Group), Phys. Lett. B **592**, 1 (2004).
- [26] I.F. Ginzburg *et al.*, Nucl. Instrum. Methods Phys. Res., Sect. A **219**, 5 (1984); V.I. Telnov, Nucl. Instrum. Methods Phys. Res., Sect. A **294**, 72 (1990).
- [27] M. Cannoni, C. Carimalo, W. Da Silva, and O. Panella, Phys. Rev. D **72**, 115004 (2005).